https://doi.org/10.5194/hess-2020-24
Preprint. Discussion started: 28 January 2020

Hydrology and Earth System Sciences
Discussions

Soil Moisture Sensor Network Design for Hydrological Applications

Lu Zhuo[1,2], Qiang Dai[2,3*], Binru Zhao[4], Dawei Han[5]

[1]Department of Civil and Structural Engineering, University of Sheffield, Sheffield, UK
[2]Key Laboratory of VGE of Ministry of Education, Nanjing Normal University, Nanjing, China
[3]Jiangsu Center for Collaborative Innovation in Geographical Information Resource Development and Application, Nanjing, China
[4]College of Water Conservancy and Hydropower Engineering, Hohai University, Nanjing, China
[5]WEMRC, Department of Civil Engineering, University of Bristol, Bristol, UK
[*]Correspondence: qd_gis@163.com

Abstract

Soil moisture plays an important role in the partitioning of rainfall into evapotranspiration, infiltration and runoff, hence a vital state variable in the hydrological modelling. However, due to the heterogeneity of soil moisture in space most existing in-situ observation networks rarely provide sufficient coverage to capture the catchment-scale soil moisture variations. Clearly, there is a need to develop a systematic approach for soil moisture network design, so that with the minimal number of sensors the catchment spatial soil moisture information could be captured accurately. In this study, a simple and low-data requirement method is proposed. It is based on the Principal Component Analysis (PCA) and Elbow curve for the determination of the optimal number of soil moisture sensors; and *K*-means Cluster Analysis (CA) and a selection of statistical criteria for the identification of the sensor placements. Furthermore, the long-term (10-year) soil moisture datasets estimated through the advanced Weather Research and Forecasting (WRF) model are used as the network design inputs. In the case of the Emilia Romagna catchment, the results show the proposed network is very efficient in estimating the catchment-scale soil moisture (i.e., with *NSE* and *r* at 0.995 and 0.999, respectively for the areal mean estimation; and 0.973 and 0.990, respectively for the areal standard deviation estimation). To retain 90% variance, a total of 50 sensors in a 22,124 km^2 catchment is needed, which in comparison with the original number of WRF grids (828 grids), the designed network requires significantly fewer sensors. However, refinements and investigations are needed to further improve the design scheme which are also discussed in the paper.

Keywords: Soil moisture network design, Principal Component Analysis (PCA), *K*-means Cluster Analysis (CA), Weather Research and Forecasting (WRF) Model, Optimising, Numerical Weather Prediction (NWP) model.

1. Introduction

Soil moisture is at the heart of the Earth system and it plays an important role in the exchanges of water and energy at the land surface (Dorigo et al., 2017;Robock et al., 2000;Crow et al., 2018). In hydrology, soil moisture is the key component for the partitioning of rainfall into evapotranspiration, infiltration and runoff (Vereecken et al., 2008;Brocca et al., 2017;Rajib et al., 2016;Fuamba et al., 2019). In particular, the antecedent soil moisture condition of a catchment is among one of the most important factors for flood triggering (Uber et al., 2018;Zhuo and Han, 2017). For hydrological modelling, soil moisture is a vital state variable. Especially, during real-time flood forecasting, the accurate updating of the soil moisture state variable is a critical step to reduce the accumulation of model errors (i.e., time drift problem) (Lopez et al., 2016;Laiolo et al., 2016;Zwieback et al., 2019). Therefore, the intensive monitoring of catchment-scale soil moisture content would benefit a number of hydrological applications.

In-situ soil moisture sensors (e.g., capacitance probe, and Time Domain Reflectometry), as one of the oldest and most common methods used around the world, can provide point-based soil moisture measurements with relatively high accuracy in comparison with the modelling and the remotely sensed approaches (Albergel et al., 2012). Therefore, they are a crucial source of information for the hydrological research (Western et al., 2004;Brocca et al., 2017). However, due to the heterogeneity of soil moisture in large space and the economic considerations, most

https://doi.org/10.5194/hess-2020-24
Preprint. Discussion started: 28 January 2020

existing in-situ networks rarely provide sufficient coverage to capture the catchment soil moisture variations (Chaney et al., 2015). In particular, in a number of cases, soil moisture sensors are mainly installed close to the residential plain areas (e.g., due to easy accessibility and maintenance reasons), and there is a lack of sensors installed in the complex topographic areas where they are really the most needed (Zhuo et al., 2019b). Therefore, there is a need to develop a systematic approach for the soil moisture network design, so that with the minimal number of sensors the catchment-scale soil moisture information could be captured accurately. However, to our knowledge, there is a lack of existing literature covering such a research area particularly for the hydrological applications (Chaney et al., 2015), albeit numerous studies have been carried out on the rain gauge network design by the community (Dai et al., 2017;Adhikary et al., 2015;Pardo-Igúzquiza, 1998;Chen et al., 2008;Bayat et al., 2019).

Therefore, to address the aforementioned research gap, the aim of this paper is to propose a pioneer soil moisture network design scheme for catchment-scale studies, based on a combination of statistical approaches. In particular, the Principal Component Analysis (PCA) and Elbow curve are adopted to determine the optimal number of soil moisture sensors within a catchment, and *K*-means Cluster Analysis (CA) and a selection of statistical criteria are used for the identification of the soil moisture sensor placements. Although the methodologies themselves are not new, it is the first time they are applied for the soil moisture network design. Furthermore, long-term (10-year) soil moisture datasets estimated through the advanced Numerical Weather Prediction (NWP) Weather Research and Forecasting (WRF) model (Skamarock et al., 2008) are used as the design inputs. WRF model has been applied in a wide range of applications with good performances (Srivastava et al., 2015;Zaitchik et al., 2013;Zhuo et al., 2019a;Stéfanon et al., 2014). Although WRF estimated soil moisture cannot represent the ground truth, they are ideal datasets to provide catchment characteristics, such as land cover, soil properties, topographies, which are the main drivers of local soil moisture heterogeneity

(Friesen et al., 2008). Therefore, such globally available datasets together with the proposed statistical approaches would provide useful insights for the soil moisture network design research (i.e., to minimise the redundancy of information, and improve accuracy), in particular, for those currently ungauged catchments. In this study, the proposed method is implemented in the Emilia Romagna region, northern Italy as a case study due to its high-exposure of flood events.

The paper is organised as: the study area is introduced in Section 2; soil moisture network design methodologies are described in Section 3; the results are presented in Section 4; and discussions and conclusions are included in Section 5.

2. Study Area

In this study, the Emilia Romagna region (latitude 43°50'N–45°00'N; longitude 9°20'E–12°40'E) is selected for the case study which is in Northern Italy (Figure 1). The region's total coverage is approximately 22,124 km^2. It is surrounded by the Apennines to the south and the Adriatic Sea to the east, with over half of the area as a plain agricultural zone (12,000 km^2). The climate condition is highly varied in the region which is largely influenced by the mountains and the sea, with subcontinental in the Po Plain and hilly areas, and cool temperate in the mountain range (Nistor, 2016). It has distinct wet and dry seasons (i.e. dry season between May and October, and wet season between November and April) (Zhuo et al., 2019b). Based on the ESA CCI land cover map (Bontemps et al., 2013), the region is mainly covered by Herbaceous (37%), followed by Tree (22%), and Cropland (21%). The majority of the area is on the quaternary alluvial deposits, which are characterised by a high degree of heterogeneity (Pistocchi et al., 2015). The annual temperature ranges from 8.2 to 19.3°C; and the annual mean precipitation is between 520 and 820 mm (Pistocchi et al., 2015).

https://doi.org/10.5194/hess-2020-24
Preprint. Discussion started: 28 January 2020

For the soil moisture network in the region, currently, there is a total of 19 soil moisture sensors installed (all located in the plain area); however only one of them can provide long-term continuous soil moisture monitoring datasets. The network is managed by the Regional Agency for Environmental Protection Emilia Romagna Region. Through further investigations, it has been found, a number of the sensors have actually never provided proper soil moisture measurements since the installation. For such a highly heterogeneous catchment, only one soil moisture sensor at the plain area is clearly not sufficient for any catchment-scale applications. Therefore, it is hoped the proposed soil moisture network design scheme could provide some useful guidance to the local authority on an improved network in the future (i.e., a minimum number of sensors for reduced installation and maintenance cost, but at the right locations).

3. Methodologies

3.1 WRF Model

The WRF model is a next-generation, non-hydrostatic mesoscale NWP system designed for both atmospheric research and operational forecasting applications (Skamarock et al., 2005). The model is capable of modelling a wide range of meteorological applications varying from tens of metres to thousands of kilometres (NCAR, 2018). Apart from the WRF's aforementioned advantage on including the catchment characteristics for the soil moisture estimations, it also has other merits that make it an ideal tool for providing the distributed soil moisture information for the network design. For instance, WRF model's spatial and temporal resolutions can be changed depending on the input datasets to fit various application requirements, and a number of globally-available data products can be selected to provide the necessary boundary and initial conditions for running the model. Therefore, WRF is able to provide valuable information for this study. Here WRF version 3.8 with the ARW dynamic core is used.

3.1.1 Model Parameterization

Apart from the atmospheric forcing, parameterization is also required to drive the WRF model. In particular, the microphysics scheme is important in simulating accurate rainfall information which in turn is significant for estimating the accurate soil moisture fluctuations. WRF V3.8 supports 23 microphysics options ranging from simple to more sophisticated mixed-phase physical options. In this study, the WRF Single-Moment 6-class scheme is adopted which considers ice, snow and graupel processes and is suitable for high-resolution applications (Zaidi and Gisen, 2018). The physical options used in the WRF setup are Dudhia shortwave radiation (Dudhia, 1989) and Rapid Radiative Transfer Model (RRTM) longwave radiation (Mlawer et al., 1997). Cumulus parameterization is based on the Kain-Fritsch scheme (Kain, 2004b) which is capable of representing sub-grid scale features of the updraft and rain processes, and such a feature is useful for real-time modelling (Gilliland and Rowe, 2007). The surface layer parameterization is based on the Revised fifth-generation Pennsylvania State University–National Center for Atmospheric Research Mesoscale Model (MM5) Monin-Obukhov scheme (Jiménez et al., 2012a). The planetary boundary layer is calculated based on the Yonsei University scheme (Hong et al., 2006a). In WRF, its land surface model plays a vital role in the integration of information generated through the surface layer scheme, the radiative forcing from the radiation scheme, the precipitation forcing from the microphysics and convective schemes, and the land surface conditions to simulate the water and energy fluxes (Ek et al., 2003). In this study, the Noah Multiparameterization (Noah-MP) is chosen, because it has shown more accurate soil moisture estimation performance than the other two main schemes (Noah and CLM4) in other studies (Cai et al., 2014;Zhuo et al., 2019a). Table 1 shows the selected WRF parameterization schemes. The static inputs (i.e., land use and soil texture) are chosen in the WRF pre-processing package. Here, the land use categorisation is interpolated from the MODIS 21-category data classified by the International Geosphere Biosphere Programme

(IGBP). The soil texture data are based on the Food and Agriculture Organization of the United Nations Global 5-minutes soil database.

3.1.2 Model Setup

The WRF model is centred over the Emilia Romagna Region, and integrates three nested domains (D1, D2, D3), with the horizontal spacing of 45 km x 45 km (outer domain, D1), 15 km x 15 km (inner domain, D2), and 5 km x 5 km (innermost domain, D3). In this study, the innermost domain D3 is used (88 x 52 grids (west-east and south-north, respectively)), with a two-way nesting scheme considered letting the information from the child domain to be fed back to the parent domain. To drive the WRF model, the European Centre for Medium-Range Weather Forecasts (ECMWF) reanalysis (ERA-Interim) is adopted to provide the study region's boundary and initial conditions. ERA-Interim is a global atmospheric reanalysis that is available from 1979 to 2019 (ERA-5 as a recent update to ERA-Interim may also be used). The spatial resolution of the datasets is approximately 80 km on 60 levels in the vertical from the surface up to 0.1 hPa. It contains 6-hourly gridded estimates of three-dimensional meteorological variables, and 3-hourly estimates of a large number of surface parameters and other two-dimensional fields. Please see (Berrisford et al., 2011) for a detailed documentation of the ERA-Interim.

After the initialization, the model needs to be spun-up to derive a physical valid state (e.g., equilibrium state) (Cai et al., 2014;Cai, 2015). In this study, WRF is spun-up by running through the whole year of 2005. After the spin-up, the WRF model is run in daily timestep from January 1, 2006, to December 31, 2015, using the ERA-Interim datasets. The modelled WRF grids within the Emilia Romagna catchment (total of 828 grids) are shown in Figure 2 as black dots, with the elevation map also illustrated in the background.

3.2 Soil Moisture Network Design

https://doi.org/10.5194/hess-2020-24
Preprint. Discussion started: 28 January 2020

For the soil moisture network design, two main problems need to be tackled. First is how many soil moisture sensors are needed within a catchment, and the second is where are the best locations to place them. To solve the first problem, the PCA is used to obtain the optimal number of soil moisture sensors through a threshold analysis. And for the second problem, the *K*-means CA is adopted to determine the locations for the sensor placements.

3.2.1. Principal Component Analysis (PCA)

When soil moisture data are collected from *p* soil moisture sensors, these data are often correlated. This correlation reflects the complexity of the catchment and indicates that some of the information collected from one sensor is also contained in the remaining *p*-1 sensors (Gangopadhyay et al., 2001). The role of the PCA is to examine the redundancy of the WRF soil moisture network, and more importantly to highlight the grids that provide the most significant contribution to the principal components (Dai et al., 2017). The optimal number of sensors is dependent on the amount of original variance the network should retain. PCA is a statistical procedure for multivariance feature extraction. It adopts an orthogonal transformation to convert a set of possibly correlated observations into a set of linearly uncorrelated variables called principal components. This transformation is defined in such a way that the first principal component has the largest possible variance, and each succeeding component in order has the highest variance possible under the constraint that it is orthogonal to the preceding components (Wold et al., 1987).

In this study, we have *p* WRF soil moisture grids with *N* observations (the time series of the data, i.e., 10-year daily datasets). The covariance matrix *p* x *p* can be calculated which is denoted as *X*, and the eigenvectors and the eigenvalues of the matrix can also be determined, correspondingly. Since the eigenvectors of the *X* are orthogonal, the *p* eigenvectors are used to construct the principal components, which can be represented as:

$$\text{eigenvector} = (eig_1 \ \ eig_2 \ eig_3 \ \dots \ eig_p) \tag{1}$$

with such a relationship, the original datasets can be transformed in terms of eigenvectors into a new dataset *Z*. *Z* is shown as the following:

$$Z_i = X_1 eig_{i,1} + X_2 eig_{i,2} + \ldots + X_p eig_{i,p} \ , \quad i = 1, \ldots, p \tag{2}$$

where Z_i is the new dataset, X_i is the original dataset. The variance of each of the component is the eigenvalue. The eigenvector with the highest eigenvalue is the principal component of the dataset. The examination of the network redundancy is implemented based on the desired rate of variance contribution, and the number of principal components can thus be calculated correspondingly. In other words, the appropriate number of soil moisture sensors are dependent on the amount of original variance the network would like to retain. If for a specific desired variance, the determined number of principal components (*k*) is significantly less than the total number of the WRF soil moisture grids (*p*), then it can be concluded that the network is heavily redundant, and even by removing a large number of grids, the remaining can still provide sufficient soil moisture information for the entire catchment; and vice versa. In this paper, the variance contribution rate of 70%~99% is tested. Generally, the required number of grids increases when the variance contribution rate increases. However, the growth rate is not constant that normally changes significantly at a critical point (threshold), which is used in this study as the desired rate for the soil moisture network design.

3.2.2. *K*-means Cluster Analysis (CA)

After deciding the optimal number of soil moisture sensors from the PCA step, CA is then applied to find the best locations for the sensors. CA is a multivariate method which aims to classify a sample of objects into a number of groups so that similar objects are placed in the same group (Everitt et al., 2001). The advantage of adopting the CA method for the network design is that there is no prior knowledge required about which objects belong to which clusters.

Because the optimal number of clusters (*k*) has already been determined by the PCA, *k*-means clustering method is utilised in this study to divide the original *p* datasets into *k* clusters. *k*-means approach is a typical distance-based clustering method which uses the distance as the indicator for similarity among objects (i.e., the smaller the distance, the higher the similarity of two objects) (Kodinariya and Makwana, 2013). In this study, the Euclidean distance is adopted as the distance measurement. It is a simple and widely used way of calculating the distances between objects in a multidimensional space (Danielsson, 1980). The centroid of each cluster is the point which the sum of Euclidean distances from all objects in that cluster is minimized. It is an iterative approach repeated for all of the clusters. Since an initial set of cluster centres is needed to be given for the CA to start, the resultant performance will be sensitive to the initial setting. In order to obtain an efficient performance, the WRF grids are ordered by their long-term mean soil moisture and the initial cluster centres are selected evenly from the new sequence (based on the number of *k* from the PCA). After which, the WRF grids are attributed to the closest cluster accordingly.

Within each of the optimised clusters, we propose two ways to find the most suitable grid for the sensor placement. One way is by finding the grid which gives the median averaged soil moisture in each of the cluster (denoted as CA-Med), and another is through identifying the maximum averaged soil moisture in each of the cluster (denoted as CA-Max) (Dai et al., 2017). As a result, for each cluster, there is one optimal grid, and grouped with the other optimal grids found in other clusters, the ideal placements for the soil moisture sensors are identified. The group of the selected grids is considered to be the optimal combination of locations that can provide the desired variance of the original WRF soil moisture measurements over the whole catchment.

3.3 Network Evaluation

Since there is no existing optimal in-situ soil moisture network that can be used as a reference for the evaluation, it is challenging to assess the designed network performance based on a comparison study. However, the designed network should be efficient enough to represent the maximum amount of information with the minimum number of sensors within a catchment. In other words, the designed network should retain the main catchment-scale soil moisture information of the original WRF network, which is particularly important for the hydrological modelling. To assess the network in such an aspect, the soil moisture information contained by the designed and the original network are compared. Two statistical indicators are used for the purpose, namely the Pearson correlation coefficient and the Nash–Sutcliffe coefficient.

The Pearson correlation coefficient (*r*) is a statistical measure of the linear correlation between two sets of datasets, which in this study can estimate the systematic deviation between the designed (R_d) and the original (R_o) catchment-scale soil moisture variations, and it is calculated by the following equation:

$$r_{R_o,R_d} = \frac{E[R_d R_O] - E[R_d]E[R_O]}{\sqrt{(E[{R_d}^2] - E[R_d]^2) \times (E[{R_O}^2] - E[R_O]^2)}} \quad (3)$$

where *E* is the mean value of the corresponding vector. In this study, the optimal performance is achieved when r_{R_o,R_d} equals to 1

Nash-Sutcliffe Efficiency (*NSE*) (Nash and Sutcliffe, 1970) is used widely in hydrology to evaluate the prediction accuracy in hydrological modelling, which can be obtained by:

$$NSE = 1 - \frac{\sum (R_o^t - R_d^t)^2}{\sum (R_o^t - E[R_o])^2} \quad (4)$$

where *t* is the time-step of the dataset. The *NSE* ranges [1,-∞). The closer *NSE* is to 1, the more accurate the designed network is.

4. Results

https://doi.org/10.5194/hess-2020-24
Preprint. Discussion started: 28 January 2020

4.1. Soil Moisture Network Redundancy Analysis

Within the study area of 22,124 km^2, there is a total number of 828 WRF soil moisture grids. With such a dense network, there should exist information redundancy. To explore this, a cross-correlation (*r*) matrix for all of the grids over the whole study period is plotted in Figure 3. It can be seen that the majority part of the map is in blue-tone, which means most of the grids (85%) are correlated ($r > 0.5$) with the others (as shown in Table 2). In addition, over half of the grids (52%) have high correlation ($r>0.8$) with the rest of the grids; and even 15% of the grids can achieve very high correlation ($r>0.9$). However, it is clear from the map some grids (e.g., grid number 396-398, 523-529) are more heterogeneous than the others (red-tone, with low correlation <0.3 observed), which means more soil moisture sensors might need to be installed in those locations. The catchment map with the indicated WRF grid numbers is presented in Figure 4a). A further exploration of cross-correlation performance using box plots is shown in Figure 4b). The locations of the selected grids (as in Figure 4b) are marked in Figure 4a) with red circles. It can be seen the nine grids are distributed evenly within the catchment in order to represent a spectrum of catchment features (e.g., different land covers, elevations, soil types etc.). From the box plot, it can be seen for a specific grid, the cross-correlation can range from as low as below 0.1 to as high as almost 1. The large range is particularly obvious for Grid 500, which is located at the plain zone near the east boundary of the catchment and is close to the Valli di Comacchio lagoon. The closeness to the waterbody could mean its soil moisture is dominated more by the waterbody than by the local weather conditions, in comparison with grids located further away. For Grid 100, its correlation with the rest of the grids in the catchment is relatively low, with 75% percentile of the cross-correlations less than 0.6. The potential reason could be because it is located in the southern mountainous zone, with high-density of tree coverage and complex topographic conditions, its soil moisture is more heterogeneous than the other grids. A similar condition is observed for

Grid 1 which is also located in a hilly zone in the southern boundary of the catchment (i.e., lower correlation as shown in the boxplots). Such a phenomenon is not unexpected and could mean more sensors are needed in those complex zones for better soil moisture monitoring purpose. However, for Grids like 300, and 600 (and the surrounding areas), since the majority of their correlations are high and they are located in plain areas with no water boundary nearby, they could be arranged with a smaller number of soil moisture sensors.

4.2. Soil Moisture Sensor Number

In summary, through the cross-correlation exploration, many parts of the WRF soil moisture network are significantly redundant, whilst for some parts, a denser network is indeed needed. To systematically investigate the redundancy degree of the network, the PCA approach is applied. Figure 5a) shows the PCA results to provide useful guidance on the acceptable loss of information. It is clear to see the first principal component carries close to 80% of the total variance, with the second component bringing this to nearly 90%. This result again indicates the high redundancy exists in the network, and just one component can contain almost 80% of the total soil moisture information. To better understand the relationship between the principal component numbers, the variance contribution rate, as well as the corresponding required grids number, a set of variance contribution rates from 70% to 97.5% is used as the representatives. The required number of components and the grids are listed accordingly in Table 3. It can be seen only one component with 6 grids is sufficient to retain 70% of the soil moisture information. Even when the variance is set at 80%, only two components are needed to meet the requirement, and the corresponding number of soil moisture girds is 11 (1.3% percent of the total grids). To satisfy 90% variance, three components are needed, and although the total number of grids is increased to 50, it is still significantly less than the WRF's full inputs. The detailed numbers further indicate the relatively high level of redundancy in the WRF's original soil moisture network.

The trend can also be observed through the Elbow curve which is illustrated in Figure 5b). It presents the relationship between the variance and the number of grids. It can be seen to meet the increment of variance, the required number of grids also increases. But the growth rate is the most significant when the variance is smaller than 70% and then slows down gradually after that. When the variance meets 95%, the rate is further weakened. Based on the curve, it is suggested the desired variance (i.e., trade-off point) between 80% and 95%. The required number of soil moisture grids for 80%, 85%, 90%, and 95% is 11, 21, 50, and 184 respectively. It is clear, in order to achieve the 95% variance, a significantly greater number of additional grids are required, that is 268% more than for the 90% variance case. Therefore, for further improvement of variance from 90% to 95%, the economic cost for the additional number of sensors might not be as valuable as for the 85% to 90% case (138% additional sensors are required for the enhancement).

4.3. Soil Moisture Sensor Location Design

Once the degree of redundancy for the full WRF soil moisture network is established, the next step is to determine the optimal locations for sensor placements. Because the components from the PCA do not directly represent the physical WRF grids, cluster analysis is thus carried out to identify the specific grid locations. Here, CA-Max and CA-Med are used. The designed networks for CA-Max and CA-Med are illustrated in Figure 6 and 7, respectively. The indicated locations in the figures provide guidance on the preferential areas for the soil moisture sensor placements. Each of the methods gives a different set of sensor locations, for instance, the selected optimal soil moisture grids from the CA-Max method tend to be located at the catchment boundary, and the situation is particularly obvious for the low variance cases (i.e., 70% - 80%). For example, when the variance is set at 70%, the selected optimal locations from the CA-Max is mostly distributed near the catchment's southern boundary, while from the CA-Med, it is more homogeneously distributed (i.e., one at the southern boundary, one at the north,

https://doi.org/10.5194/hess-2020-24
Preprint. Discussion started: 28 January 2020

two at the north-western part, and two at the north-eastern part). When the variance is increased, for instance at 90%, the difference between the two CA methods becomes less distinctive. Despite this, it can still be seen for the CA-Max, there is less coverage of sensors at the western and the eastern parts of the catchment, with most of the sensors located at the mid-region. However, for the same variance, the sensor distribution from the CA-Med looks more evenly distributed visually. Nevertheless, when the variance reaches as high as 97.5%, the difference from the two methods becomes rather small, as 367 sensors are located covering most parts of the catchment in both cases.

4.4. Soil Moisture Network Evaluation

The evaluation of the designed network is challenging, as there are no standard assessment criteria available to guide on what kind of network is the most appropriate for a given study area. In essence, the designed network should be efficient, which means the network should contain the maximum amount of information with a minimal number of sensors. In this study since we focus on the soil moisture's hydrological applications (catchment-scale), to evaluate the efficiency of the proposed schemes, the catchment-scale soil moisture data derived by the designed networks are compared with the WRF's full inputs (828 grids). Both the areal spatial mean and standard deviation are calculated. The Pearson correlation coefficient and the Nash–Sutcliffe coefficient are used to quantify the relationships between the two soil moisture datasets. The results for both the CA-Med and the CA-Max are compared in Figure 8. Based on the areal mean soil moisture (Figure 8 a) and c)), it is clear to see the CA-Med outperforms the CA-Max for the majority of the variance cases (both *NSE* and *r*), except for the *NSE* results when the variance is over 90%. Moreover, for the *NSE* results, a decline of the performance can be observed clearly after it passes the 90% variance point, which illustrates that an increment of sensor number does not necessarily mean a arise of the performance. For the standard deviation, the disparity between the two methods is smaller. When the variance is below 80%, the growth trend for the CA-Med case is not clear, as it firstly drops at the 75% point and then climbs up again when the variance increases. Whereas for the CA-Max case, there is a clear upward trend. Similar to Figure 8 a), it is interesting to see for the areal standard deviation in Figure 8 b) and d), the *NSE* and *r* also start to drop after reaching around 90%, which again indicates the increment of sensor number does not positively link to the improvement of network performance (here in the aspect of spatial variation). The evaluation results are summarised in Table 4 for numerical comparison. Since CA-Med surpasses CA-Max for most of the cases, it is chosen for the network design. In the aspect of the desired variance, because as discussed earlier, when the variance climbs over 90%, the performance instead drops. Therefore 90% variance is suitable to be used for the network design in this case.

The time series plots of the areal soil moisture mean and standard deviation are shown in Figure 9. Generally, the designed network can estimate the catchment's mean soil moisture very well, as it follows the variation of the WRF's full input dataset closely (*NSE* = 0.995 and *r* = 0.999). For the standard deviation, the general trend from both datasets shows a higher spatial variation of soil moisture over the dry season and lower variation during the wet season. The spatial variation is averaged around 0.04 m^3/m^3 throughout the whole study period. However, there are some disparities between the two datasets, in particular, during the wet season (bottom peaks in the STD plot), the designed network at several occasions overestimates the spatial soil moisture variation, and during the dry season (top peaks in the STD plot), it underestimates instead. Nevertheless, the differences are small and the correlation between the two datasets is high, with *NSE* = 0.973 and *r* = 0.990 obtained. In conclusion, the designed network can maintain the dominated information of the WRF's full-grid input well.

The sensor displacements for the designed and the existing (in-situ) networks are illustrated in Figure 10. In comparison with the distribution of the proposed network, the existing network is clearly biased, with all of the sensors located in the mid-plain zone only. Such distribution

https://doi.org/10.5194/hess-2020-24
Preprint. Discussion started: 28 January 2020

(i.e., no sensors located at the southern mountainous (highly-vegetated) region) can have adverse impacts on the accuracy of the areal mean soil moisture estimation. Scatterplots of the areal mean soil moisture calculated from the designed and the existing networks are also presented in Figure 11. The performance difference between the two networks is clear to observe. For the proposed network, the points are located close to the identical line, whereas for the existing network, due to the inappropriate sensor distributions over the catchment, the points are more dispersive (*NSE* = 0.889). The performance of the existing network in comparison with the proposed networks indicates that it cannot retain even 70% of the variance (as compared with the *NSE* results in Table 4), as the *NSE* for the 70% CA-Med can achieve 0.949. For the existing network, without putting sensors in the highly vegetated region, the network clearly underestimates soil moisture variations during the dry season (i.e., for the cases when the soil moisture is less than 0.25 m^3/m^3)

5. Discussions and conclusions

With the low-cost soil moisture sensors becoming more and more available and modern communication technology (i.e., Internet of Things), it is expected more in-situ soil moisture sensors will be installed in the future. However, unlike the rich literature in the rain gauge network design field, there is a research gap in soil moisture network design for catchment-scale applications. As a result, research is urgently needed to fill this important knowledge gap. As one of the pioneering studies in this field, a low-data requirement method is proposed in this study for the in-situ soil moisture network design. Through a series of evaluations of the developed network, it can be concluded that the method can provide efficient catchment-scale soil moisture estimations (i.e., high accuracy of the areal mean and standard deviation soil moisture estimations). To retain 90% variance, a total of 50 sensors in a 22,124 km^2 catchment is needed. In comparison with the original number of WRF's grids (828 grids), the proposed network requires significantly smaller number of sensors. Furthermore, in comparison with the existing soil moisture network in the Emilia Romagna region, the proposed network has sensors more evenly distributed, covering most representative parts of the catchment (e.g., both plain and mountainous regions), and can obtain more accurate catchment-scale soil moisture estimation. However, there are several points need to be discussed as follows.

The first point is about the uncertainty of the WRF's soil moisture estimations, which could influence the accuracy of the network design. It is acknowledged that the reliability of the designed network is influenced by the performance of the WRF model. To evaluate the WRF results and test whether the proposed network can produce the catchment-scale soil moisture well, a long-term densely covered soil moisture network will be required. Setting up such a network is challenging and difficult to realise due to the high installation and maintenance cost. In this study, a long-term WRF soil moisture estimation with 1-year spin-up time is used which could to some extent produce a more stable result. But since "all models are wrong" (by George E. P. Box), an uncertainty model (Zhuo et al., 2016) could be proposed to be integrated with the network design scheme. For example, we can generate a large number of probable "true soil moisture" datasets based on the proposed uncertainty model so that a set of possible soil moisture networks can be produced. As a result, the designed network will be expressed in a probabilistic form instead of a determinate form. In addition, a decision-making scheme considering different conditions (e.g., accessibility, installation and maintenance cost) under the uncertainty can be developed to select the most suitable soil moisture network. The uncertainty influence of the WRF soil moisture on the network design will be investigated in future studies.

Second, the case study is based on the daily soil moisture inputs for the hydrological applications. With different research needs (meteorology, climatology, hydrology, water resources, geology, etc.), various temporal-scale of soil moisture data might be required, for example, climate change study requires soil moisture data in decades or hundreds of years which often needs annual-scale measurements; drought assessment requires monthly to seasonal datasets; while for hydrometeorological prediction applications, hourly datasets might be needed. For the network design, the input data's temporal scale (daily, weekly, monthly, yearly) can influence the final network design, therefore it is worth investigating in future studies about the temporal-scale effect on the network design.

Third, for a complex catchment like Emilia Romagna, other uncertainty sources apart from the WRF model can also affect the performance of the designed network; for instance, the study area has varied climate conditions (a mixture of subcontinental and cool temperate) and distinct seasonal changes (wet/dry seasons). Therefore separating/combining networks under different catchment conditions could result in an improved soil moisture network design. Furthermore, the poor accessibility to sensors is another challenging point that can hamper the performance of the designed network in real life, for instance, even an in-situ network follows tightly through a systematic design scheme, without proper maintenance due to the accessibility issue, the quality of the retrieved data can be highly affected. Therefore, the accessibility factor should also be considered for the network design (e.g., can be considered during the CA for the sensor placements).

Since the forcing data for the WRF model is globally covered, the proposed scheme can largely benefit ungauged catchments. On the other hand, in places where dense soil moisture networks are already available, the proposed scheme could also help in minimizing the cost by reducing the number of sensors. Another advantage of the method is that the number of soil moisture sensors can be changed based on different variances to meet various requirements. Through selecting different variance levels, the redundancy of the WRF's full-input network can be assessed, and the corresponding optimal sensor number can be determined. However, the proposed scheme is still in its infancy with a lot of refinements and further explorations needed, therefore it is hoped this paper will stimulate more studies by the community in tackling the soil moisture network design problem.

Acknowledgement

This research is supported by the National Natural Science Foundation of China (NSFC, grant no. 41871299), and Resilient Economy and Society by Integrated SysTems modelling (RESIST), Newton Fund via Natural Environment Research Council (NERC) and Economic and Social Research Council (ESRC) (NE/N012143/1).

References

Adhikary, S. K., Yilmaz, A. G., and Muttil, N.: Optimal design of rain gauge network in the Middle Yarra River catchment, Australia, Hydrol. Process., 29, 2582-2599, 2015.

Albergel, C., De Rosnay, P., Gruhier, C., Muñoz-Sabater, J., Hasenauer, S., Isaksen, L., Kerr, Y., and Wagner, W.: Evaluation of remotely sensed and modelled soil moisture products using global ground-based in situ observations, Remote Sens. Environ., 118, 215-226, 2012.

Bayat, B., Hosseini, K., Nasseri, M., and Karami, H.: Challenge of rainfall network design considering spatial versus spatiotemporal variations, J. Hydrol., 574, 990-1002, 2019.

Berrisford, P., Dee, D., Poli, P., Brugge, R., Fielding, K., Fuentes, M., Kallberg, P., Kobayashi, S., Uppala, S., and Simmons, A.: The ERA-Interim archive, version 2.0, https://www.ecmwf.int/node/8174, 2011.

Bontemps, S., Defourny, P., Radoux, J., Van Bogaert, E., Lamarche, C., Achard, F., Mayaux, P., Boettcher, M., Brockmann, C., and Kirches, G.: Consistent global land cover maps for climate modelling communities: Current achievements of the ESA's land cover CCI, Proceedings of the ESA Living Planet Symposium, Edimburgh, 2013, 9-13,

Brocca, L., Ciabatta, L., Massari, C., Camici, S., and Tarpanelli, A.: Soil moisture for hydrological applications: open questions and new opportunities, Water, 9, 140, 2017.

Cai, X., Yang, Z. L., Xia, Y., Huang, M., Wei, H., Leung, L. R., and Ek, M. B.: Assessment of simulated water balance from Noah, Noah - MP, CLM, and VIC over CONUS using the NLDAS test bed, J. Geophys. Res. Atmos., 119, 13,751-713,770, 2014.

Cai, X.: Hydrological assessment and biogeochemical advancement of the Noah-MP land surface model, Doctor of Philosophy, Geological Sciences, The University of Texas at Austin, 164 pp., 2015.

Chaney, N. W., Roundy, J. K., Herrera-Estrada, J. E., and Wood, E. F.: High-resolution modeling of the spatial heterogeneity of soil moisture: Applications in network design, Water Resour. Res., 51, 619-638, 2015.

Chen, F., and Dudhia, J.: Coupling an advanced land surface-hydrology model with the Penn State-NCAR MM5 modeling system. Part I: Model implementation and sensitivity, Monthly Weather Review, 129, 569-585, 2001.

Chen, Y. C., Wei, C., and Yeh, H. C.: Rainfall network design using kriging and entropy, Hydrol. Process., 22, 340-346, 2008.

Crow, W., Chen, F., Reichle, R., Xia, Y., and Liu, Q.: Exploiting soil moisture, precipitation, and streamflow observations to evaluate soil moisture/runoff coupling in land surface models, Geophys. Res. Lett., 45, 4869-4878, 2018.

Dai, Q., Bray, M., Zhuo, L., Islam, T., and Han, D.: A scheme for rain gauge network design based on remotely sensed rainfall measurements, J. Hydrometeorol., 18, 363-379, 2017.

Danielsson, P.-E.: Euclidean distance mapping, Computer Graphics and Image Processing, 14, 227-248, 1980.

Dorigo, W., Wagner, W., Albergel, C., Albrecht, F., Balsamo, G., Brocca, L., Chung, D., Ertl, M., Forkel, M., and Gruber, A.: ESA CCI Soil Moisture for improved Earth system understanding: State-of-the art and future directions, Remote Sens. Environ., 203, 185-215, 2017.

Dudhia, J.: Numerical study of convection observed during the winter monsoon experiment using a mesoscale two-dimensional model, Journal of the Atmospheric Sciences, 46, 3077-3107, 1989.

Ek, M., Mitchell, K., Lin, Y., Rogers, E., Grunmann, P., Koren, V., Gayno, G., and Tarpley, J.: Implementation of Noah land surface model advances in the National Centers for Environmental Prediction operational mesoscale Eta model, J. Geophys. Res. Atmos., 108, 2003.

Everitt, B., Landau, S., and Leese, M.: Cluster Analysis 4th Edition,, Taylor & Francis, London, 2001.

Friesen, J., Rodgers, C., Oguntunde, P. G., Hendrickx, J. M., and van de Giesen, N.: Hydrotope-based protocol to determine average soil moisture over large areas for satellite calibration and validation with results from an observation campaign in the Volta Basin, West Africa, IEEE T Geosci Remote, 46, 1995-2004, 2008.

Fuamba, M., Branger, F., Braud, I., Batchabani, E., Sanzana, P., Sarrazin, B., and Jankowfsky, S.: Value of distributed water level and soil moisture data in the evaluation of a distributed hydrological model: Application to the PUMMA model in the Mercier catchment (6.6 km2) in France, J. Hydrol., 569, 753-770, 2019.

Gangopadhyay, S., Das Gupta, A., and Nachabe, M.: Evaluation of ground water monitoring network by principal component analysis, Groundwater, 39, 181-191, 2001.

Gilliland, E. K., and Rowe, C. M.: A comparison of cumulus parameterization schemes in the WRF model, Proceedings of the 87th AMS Annual Meeting & 21th Conference on Hydrology, 2007,

Hong, S.-Y., Noh, Y., and Dudhia, J.: A new vertical diffusion package with an explicit treatment of entrainment processes, Mon. Weather Rev., 134, 2318-2341, 2006a.

Hong, S.-Y., Noh, Y., and Dudhia, J.: A new vertical diffusion package with an explicit treatment of entrainment processes, Monthly Weather Review, 134, 2318-2341, 2006b.

Jiménez, P. A., Dudhia, J., González-Rouco, J. F., Navarro, J., Montávez, J. P., and García-Bustamante, E.: A revised scheme for the WRF surface layer formulation, Mon. Weather Rev., 140, 898-918, 2012a.

Jiménez, P. A., Dudhia, J., González-Rouco, J. F., Navarro, J., Montávez, J. P., and García-Bustamante, E.: A revised scheme for the WRF surface layer formulation, Monthly Weather Review, 140, 898-918, 2012b.

Kain, J. S.: The Kain-Fritsch convective parameterization: An update, Journal of Applied Meteorology, 43, http://dx.doi.org/10.1175/1520-0450(2004)043<0170:TKCPAU>2.0.CO;2, 2004a.

Kain, J. S.: The Kain-Fritsch convective parameterization: An update, J. Appl. Meteorol., 43, http://dx.doi.org/10.1175/1520-0450(2004)043<0170:TKCPAU>2.0.CO;2, 2004b.

Kodinariya, T. M., and Makwana, P. R.: Review on determining number of Cluster in K-Means Clustering, Int. J. Adv. Res. Comput. Sci. Manag. Stud., 1, 90-95, 2013.

Laiolo, P., Gabellani, S., Campo, L., Silvestro, F., Delogu, F., Rudari, R., Pulvirenti, L., Boni, G., Fascetti, F., and Pierdicca, N.: Impact of different satellite soil moisture products on the predictions of a continuous distributed hydrological model, Int J Appl Earth Obs, 48, 131-145, 2016.

Lopez, P. L., Wanders, N., Schellekens, J., Renzullo, L. J., Sutanudjaja, E. H., and Bierkens, M. F.: Improved large-scale hydrological modelling through the assimilation of streamflow and downscaled satellite soil moisture observations, Hydrol. Earth Syst. Sci., 20, 3059-3076, 2016.

Mlawer, E. J., Taubman, S. J., Brown, P. D., Iacono, M. J., and Clough, S. A.: Radiative transfer for inhomogeneous atmospheres: RRTM, a validated correlated-k model for the longwave, Journal of Geophysical Research: Atmospheres, 102, 16663-16682, 1997.

Nash, J. E., and Sutcliffe, J. V.: River flow forecasting through conceptual models part I—A discussion of principles, J. Hydrol., 10, 282-290, 1970.

Weather research and forcasting model, 2018.

Nistor, M. M.: Spatial distribution of climate indices in the Emilia‐Romagna region, Meteorol. Appl., 23, 304-313, 2016.

Pardo-Igúzquiza, E.: Optimal selection of number and location of rainfall gauges for areal rainfall estimation using geostatistics and simulated annealing, J. Hydrol., 210, 206-220, 1998.

Pistocchi, A., Calzolari, C., Malucelli, F., and Ungaro, F.: Soil sealing and flood risks in the plains of Emilia-Romagna, Italy, J. Hydrol. Reg. Stud., 4, 398-409, 2015.

Rajib, M. A., Merwade, V., and Yu, Z.: Multi-objective calibration of a hydrologic model using spatially distributed remotely sensed/in-situ soil moisture, J. Hydrol., 536, 192-207, 2016.

Robock, A., Vinnikov, K. Y., Srinivasan, G., Entin, J. K., Hollinger, S. E., Speranskaya, N. A., Liu, S., and Namkhai, A.: The global soil moisture data bank, Bull. Amer. Meteor. Soc., 81, 1281-1300, 2000.

Skamarock, W., Klemp, J., Dudhia, J., Gill, D., Barker, D., Duda, M., Huang, X., Wang, W., and Powers, J.: A description of the advanced research WRF Version 3, NCAR technical note, Mesoscale and Microscale Meteorology Division, National Center for Atmospheric Research, Boulder, Colorado, USA, 2008.

Skamarock, W. C., Klemp, J. B., Dudhia, J., Gill, D. O., Barker, D. M., Wang, W., and Powers, J. G.: A description of the advanced research WRF version 2, National Center for Atmospheric Research Boulder, Colorado, USA, 2005.

Srivastava, P. K., Han, D., Rico-Ramirez, M. A., O'Neill, P., Islam, T., Gupta, M., and Dai, Q.: Performance evaluation of WRF-Noah Land surface model estimated soil moisture for hydrological application: Synergistic evaluation using SMOS retrieved soil moisture, J. Hydrol., 529, 200-212, 2015.

Stéfanon, M., Drobinski, P., D'Andrea, F., Lebeaupin-Brossier, C., and Bastin, S.: Soil moisture-temperature feedbacks at meso-scale during summer heat waves over Western Europe, Clim. Dyn., 42, 1309-1324, 2014.

Thompson, G., Field, P. R., Rasmussen, R. M., and Hall, W. D.: Explicit forecasts of winter precipitation using an improved bulk microphysics scheme. Part II: Implementation of a new snow parameterization, Monthly Weather Review, 136, 5095-5115, 2008.

Uber, M., Vandervaere, J.-P., Zin, I., Braud, I., Heisterman, M., Legoût, C., Molinié, G., and Nord, G.: How does initial soil moisture influence the hydrological response? A case study from southern France, Hydrol. Earth Syst. Sci., 22, 6127-6146, 2018.

Vereecken, H., Huisman, J., Bogena, H., Vanderborght, J., Vrugt, J., and Hopmans, J. W.: On the value of soil moisture measurements in vadose zone hydrology: A review, Water Resour. Res., 44, 2008.

Western, A. W., Zhou, S.-L., Grayson, R. B., McMahon, T. A., Blöschl, G., and Wilson, D. J.: Spatial correlation of soil moisture in small catchments and its relationship to dominant spatial hydrological processes, J. Hydrol., 286, 113-134, 2004.

Wold, S., Esbensen, K., and Geladi, P.: Principal component analysis, Chemometr Intell Lab Syst 2, 37-52, 1987.

Zaidi, S. M., and Gisen, J. I. A.: Evaluation of Weather Research and Forecasting (WRF) Microphysics single moment class-3 and class-6 in Precipitation Forecast, MATEC Web of Conferences, 2018, 03007,

Zaitchik, B. F., Santanello, J. A., Kumar, S. V., and Peters-Lidard, C. D.: Representation of soil moisture feedbacks during drought in NASA unified WRF (NU-WRF), J. Hydrometeorol., 14, 360-367, 2013.

Zhuo, L., Dai, Q., Islam, T., and Han, D.: Error distribution modelling of satellite soil moisture measurements for hydrological applications, Hydrol. Process., 30, 2223-2236, 2016.

Zhuo, L., and Han, D.: Multi-source hydrological soil moisture state estimation using data fusion optimisation, Hydrol. Earth Syst. Sci., 21, 3267-3285, 2017.

Zhuo, L., Dai, Q., Han, D., Chen, N., and Zhao, B.: Assessment of simulated soil moisture from WRF Noah, Noah-MP, and CLM land surface schemes for landslide hazard application, Hydrol. Earth Syst. Sci., 23, 4199-4218, 2019a.

Zhuo, L., Dai, Q., Han, D., Chen, N., Zhao, B., and Berti, M.: Evaluation of Remotely Sensed Soil Moisture for Landslide Hazard Assessment, IEEE J-STARS, 12, 162-173, 2019b.

Zwieback, S., Westermann, S., Langer, M., Boike, J., Marsh, P., and Berg, A.: Improving permafrost modeling by assimilating remotely sensed soil moisture, Water Resour. Res., 55, 1814-1832, 2019.

https://doi.org/10.5194/hess-2020-24
Preprint. Discussion started: 28 January 2020

Table 1. WRF parameterizations used in this study.

	Settings/ Parameterizations	References
Map projection	Lambert	
Central point of domain	Latitude: 44.54; Longitude: 11.02	
Latitudinal grid length	5 km	
Longitudinal grid length	5 km	
Model output time step	Daily	
Nesting	Two-way	
Land surface model	Noah-MP	
Simulation period	1/1/2006 – 31/12/2015	
Spin-up period	1/1/2005 – 31/12/2005	
Microphysics	New Thompson	(Thompson et al., 2008)
Shortwave radiation	Dudhia scheme	(Dudhia, 1989)
Longwave radiation	Rapid Radiative Transfer Model	(Mlawer et al., 1997)
Surface layer	Revised MM5	(Jiménez et al., 2012b;Chen and Dudhia, 2001)
Planetary boundary layer	Yonsei University method	(Hong et al., 2006b)
Cumulus Parameterization	Kain-Fritsch (new Eta) scheme	(Kain, 2004a)

Table 2. The relationship between the percentage of grids, and the cross-correlation.

Cross-correlation (*r*)	Percentage of grids (%)
0.5	85
0.6	78
0.7	70
0.8	52
0.9	15
0.95	3

Table 3. The number of components and grids to reach % variance threshold (based on the PCA method and the Elbow curve method).

Variance (%)	Components	Number of grids
70.0	1	6
75.0	1	7
80.0	2	11
85.0	2	21
90.0	3	50
92.5	3	94
95.0	3	184
97.5	3	367

Table 4. *NSE* and correlation *r* performance of CA_Med and CA_Max.

Variance	CA_Max_Mean		CA_Med_Mean		CA_Max_STD		CA_Med_STD	
	NSE	r	NSE	r	NSE	r	NSE	r
70.0	0.831	0.978	0.949	0.985	0.601	0.834	0.716	0.876
75.0	0.851	0.984	0.978	0.993	0.778	0.887	0.746	0.870
80.0	0.894	0.990	0.991	0.996	0.867	0.945	0.901	0.951
85.0	0.976	0.997	0.991	0.998	0.926	0.967	0.930	0.976
90.0	0.988	0.998	**0.995**	**0.999**	0.963	0.986	**0.973**	**0.990**
92.5	0.997	0.998	0.990	0.999	0.969	0.989	0.960	0.992
95.0	0.994	0.999	0.985	0.999	0.932	0.990	0.914	0.986
97.5	0.988	1.000	0.983	1.000	0.910	0.986	0.895	0.982

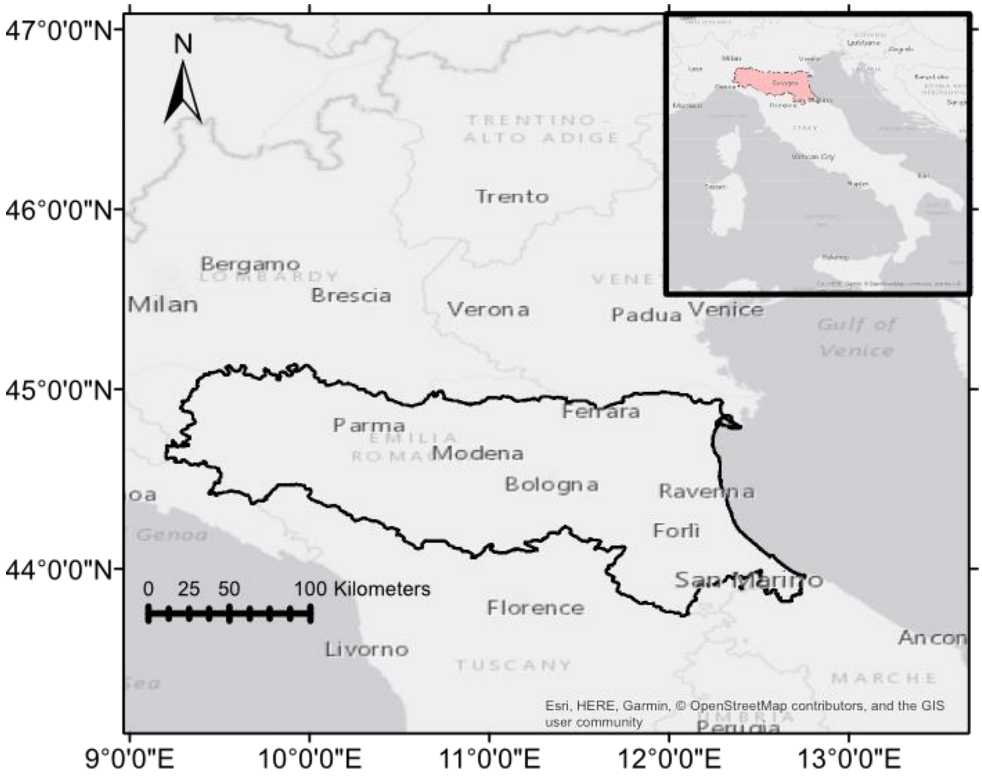

Esri, HERE, Garmin, © OpenStreetMap contributors, and the GIS user community

Figure 1. The geographical map of the Emilia Romagna region.

651 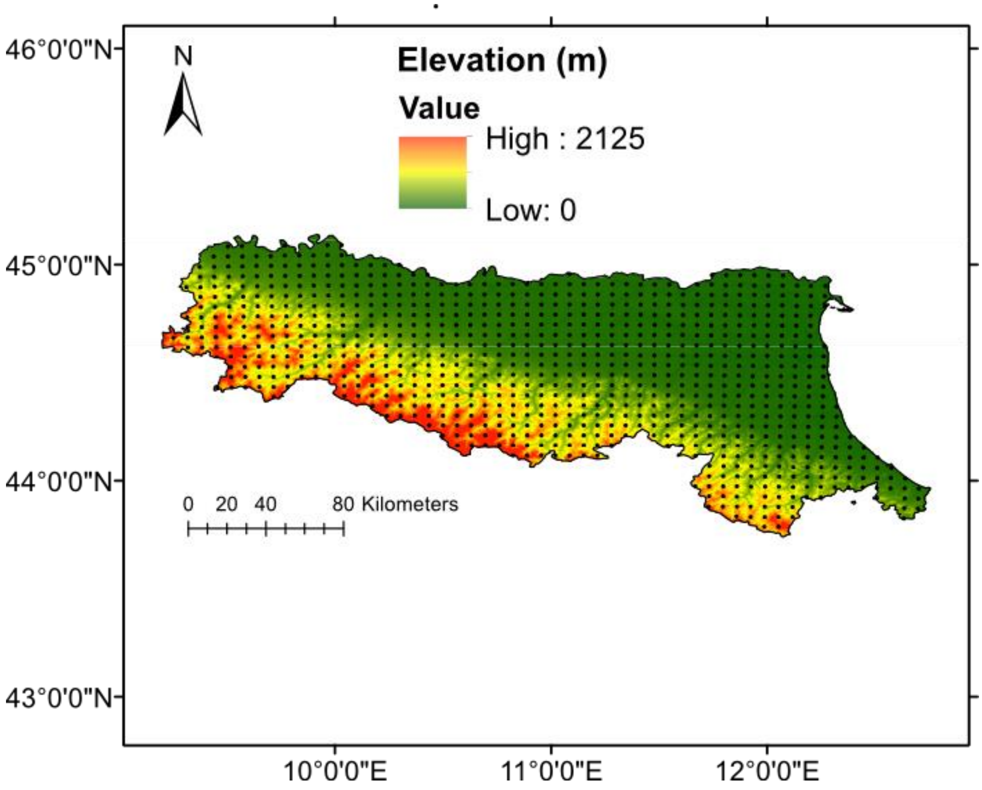

652

653 **Figure 2.** WRF grids used in the analysis, with DEM map in the background.

654

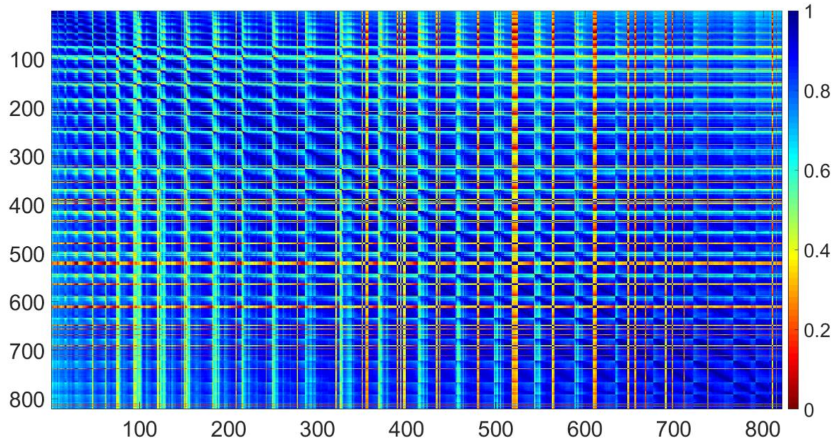

Figure 3. Cross correlation matrix for the whole catchment.

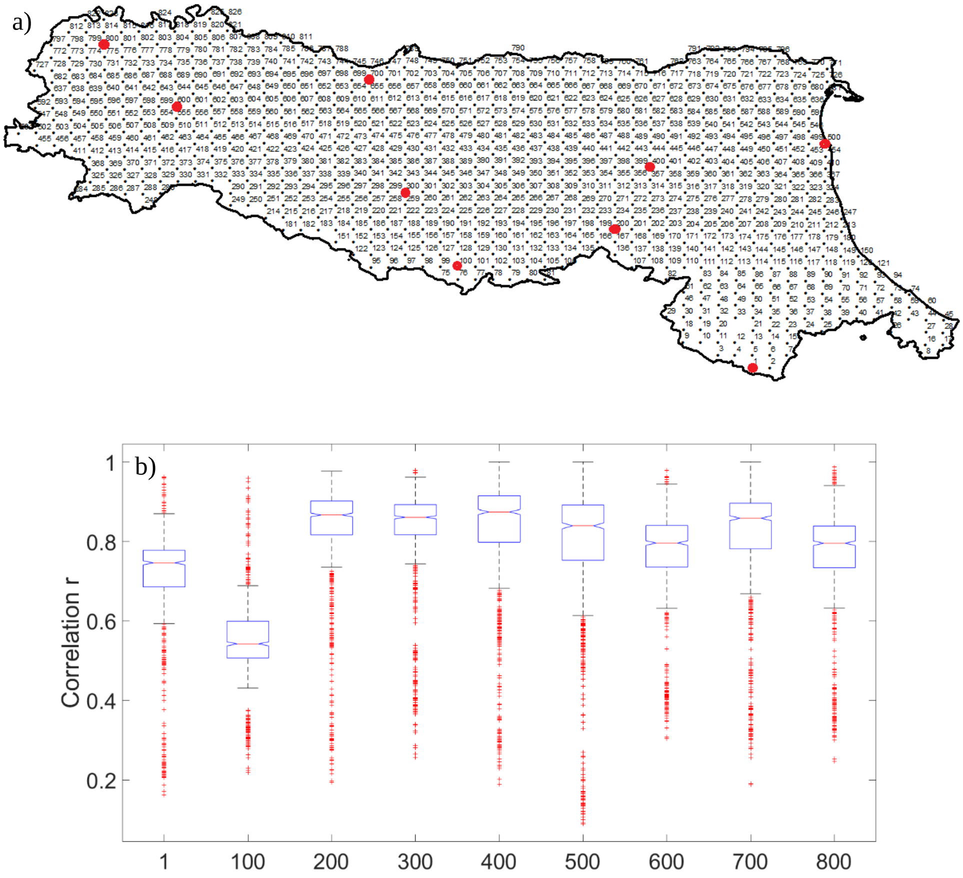

Figure 4. a) WRF grid number; b) correlation boxplot for the selected grids as highlighted in red in a). For the boxplot, it shows the minimum, maximum, 0.25, 0.50, and 0.75 percentiles and outliers (red cross).

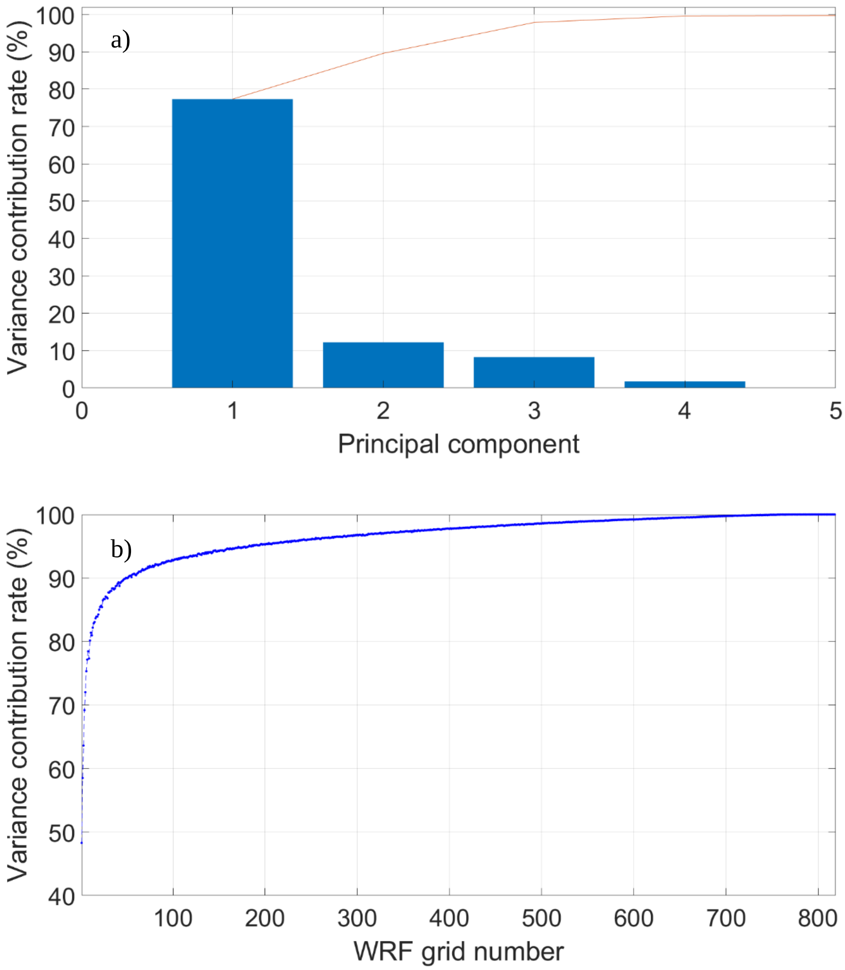

Figure 5. a) PCA analysis; b) Elbow curve.

https://doi.org/10.5194/hess-2020-24
Preprint. Discussion started: 28 January 2020

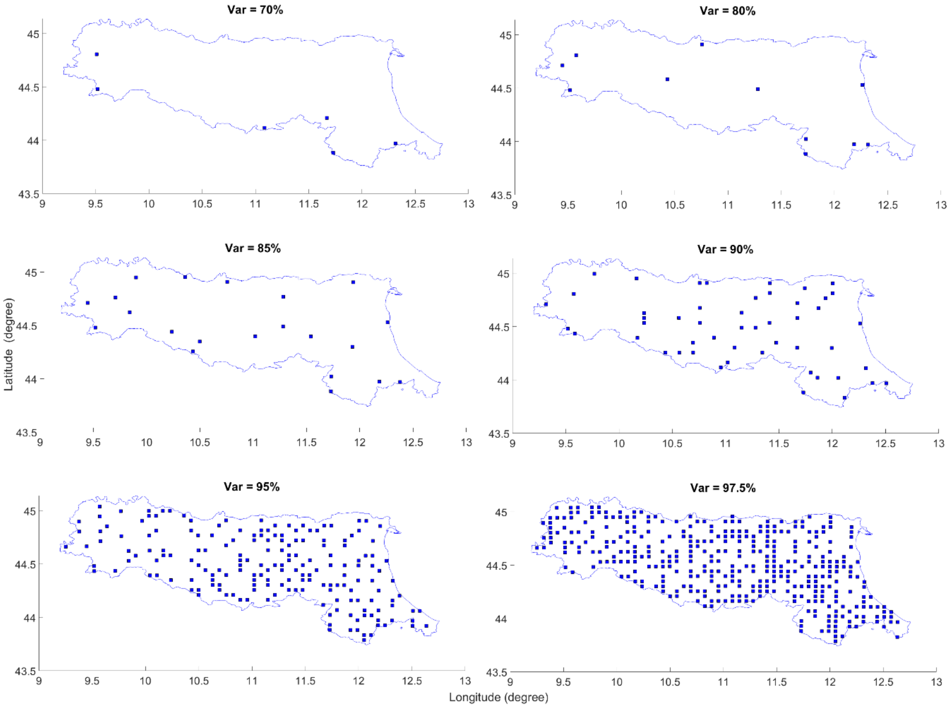

678

679 **Figure 6.** Designed soil moisture sensor locations, based on CA-Max.

680

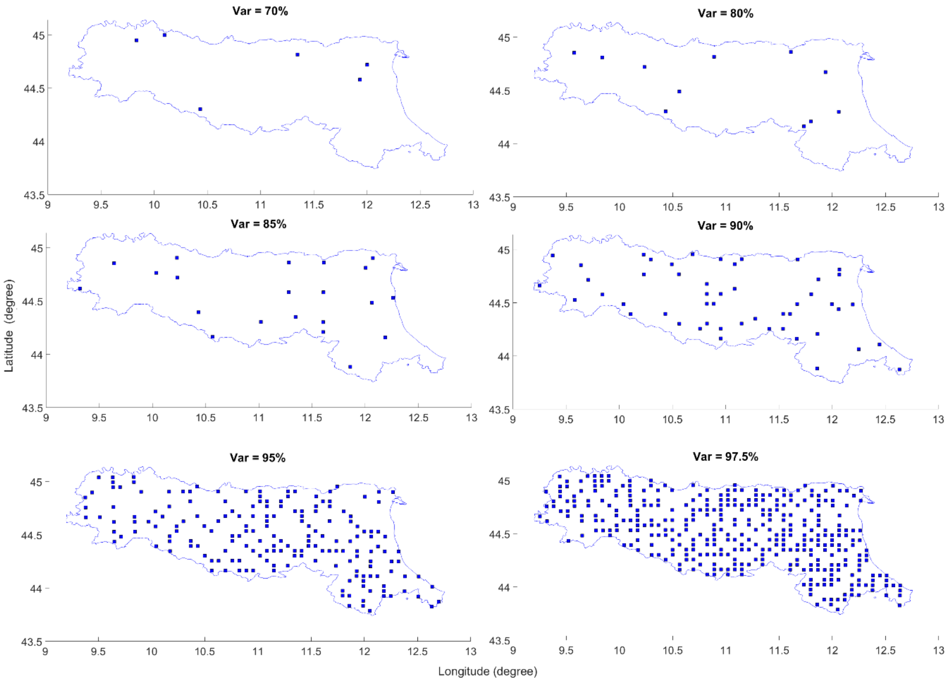

Figure 7. Designed soil moisture sensor locations, based on CA-Med.

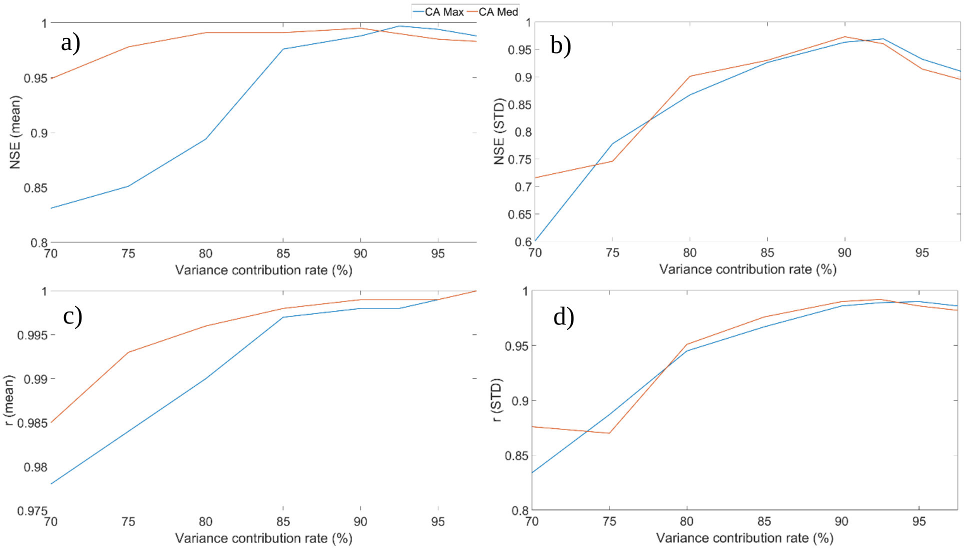

Figure 8. *NSE* and *r* plots: a) *NSE* performance based on the areal mean soil moisture, b) *NSE* performance based on the areal standard deviation soil moisture (STD), c) *r* performance based on the areal mean soil moisture, d) *r* performance based on the areal standard deviation soil moisture.

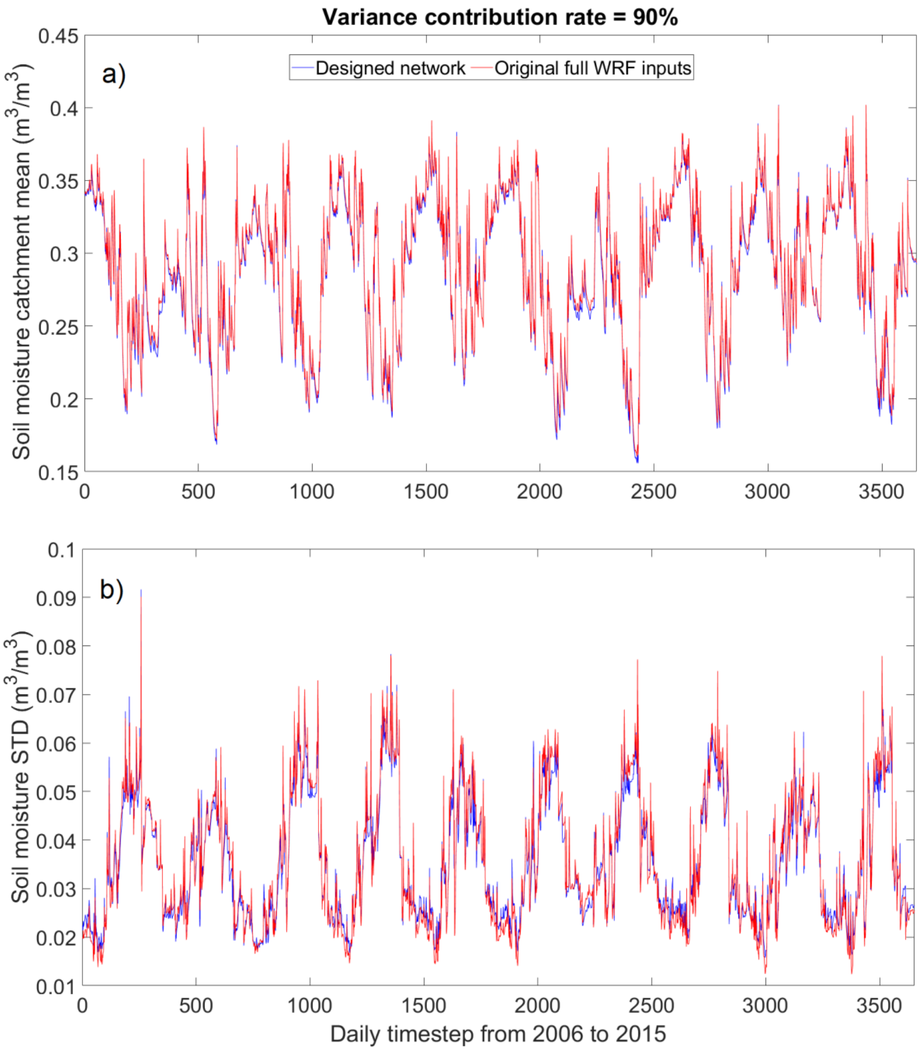

Figure 9. a) The areal mean soil moisture of the designed and the WRF's full-input networks, b) the areal soil moisture standard deviation of the designed and the WRF's full-input networks.

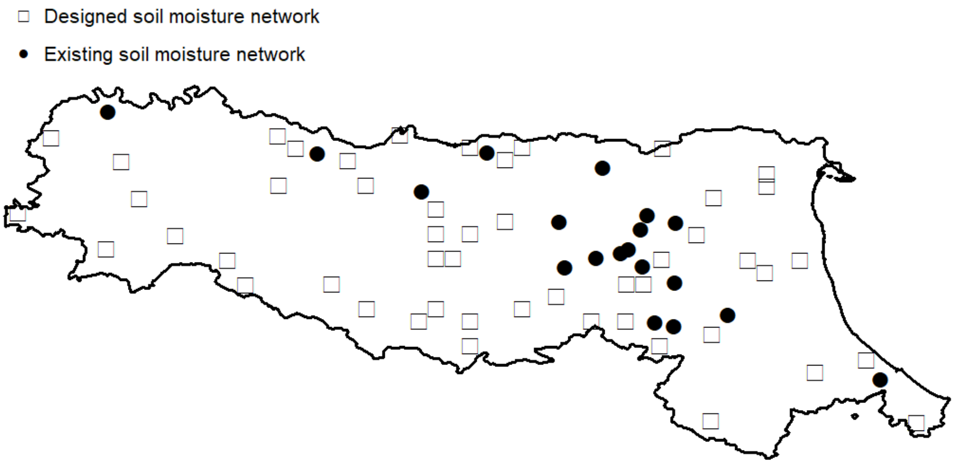

Figure 10. Comparison between the existing and the designed soil moisture networks.

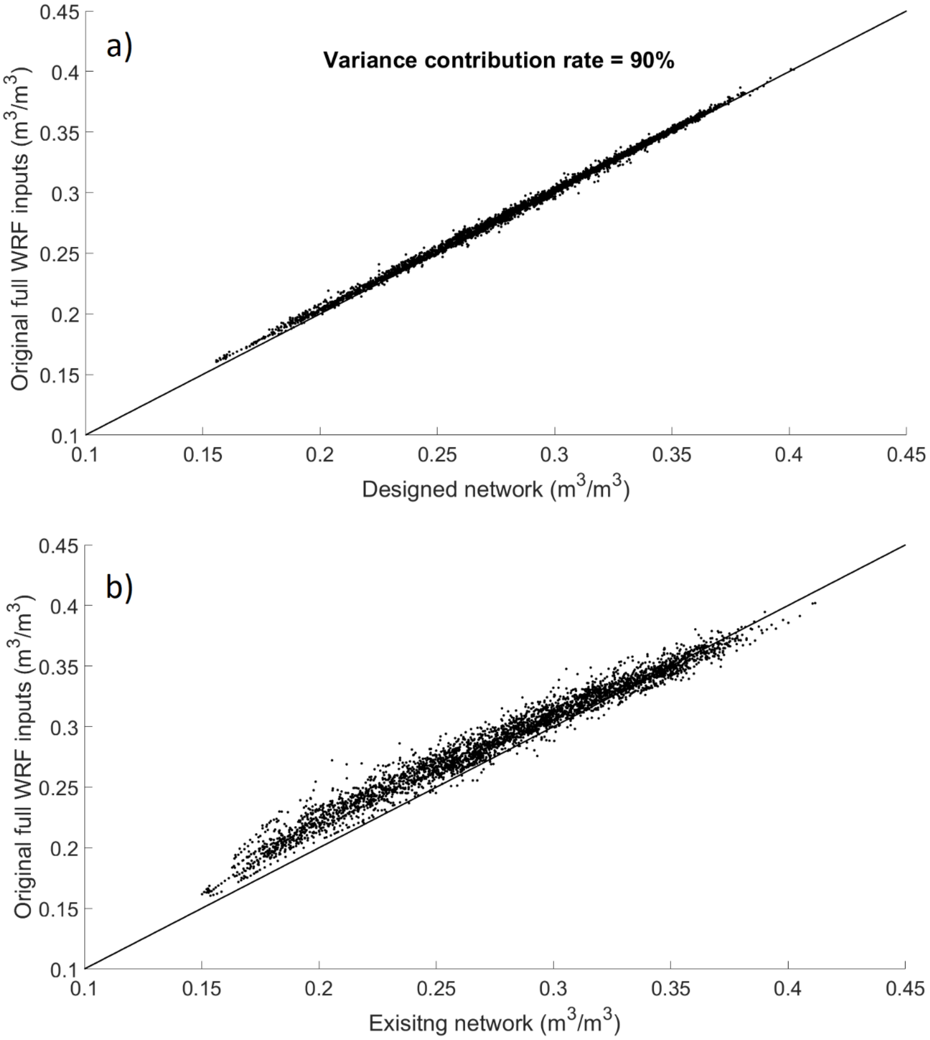

Figure 11. Scatterplots for areal mean soil moisture: a) WRF full grid inputs against the proposed network (*NSE* = 0.995, *r* = 0.998); b) WRF full grid inputs against the existing in-situ network (*NSE* = 0.889, *r* = 0.987).